Ethylene Oxide Monitor with Part-per-Trillion Precision for In-Situ Measurements

Tara I. Yacovitch, Christoph Dyroff, Joseph R. Roscioli, Conner Daube, J. Barry McManus, Scott C. Herndon

Aerodyne Research, Inc., 45 Manning Road, Billerica, Massachusetts, 01821 USA

Correspondence to: Tara I. Yacovitch (tyacovitch@aerodyne.com)

Abstract. An Aerodyne Tunable Infrared Direct Absorption Spectrometer with a multipass cell with 413 meter pathlength for the detection of ethylene oxide (EtO) is presented (TILDAS-FD-EtO). This monitor achieves precisions of <75 ppt or <0.075 ppb in 1 second and < 20 ppt in 100 seconds (1-sigma). We demonstrate precisions averaging down to 4 ppt in an hour (1-sigma precision) when operated with frequent humidity-matched zeroes. A months-long record of 2022 ambient concentrations at a site in the Eastern United States is presented. Average ambient EtO concentration is on the order of 18 ppt (22 ppt standard deviation). Enhancement events of EtO lasting a few hours are observed, with peaks as high as 600 ppt. Back trajectory simulations suggest an EtO source nearly 35 km away. This source along with another are confirmed as emitters through mobile near-source measurements, with downwind concentrations in the 0.5 ppb to 700 ppb range depending on source identity and distance downwind.

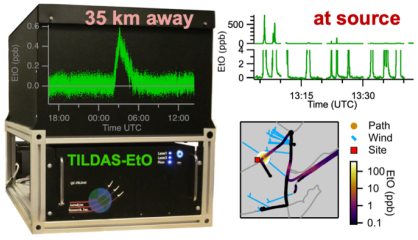

1 Introduction

Ethylene oxide (EtO, also known as EO or oxirane) is a reactive compound with a strained 3-member ether ring (C_2H_4O, CAS# 75-21-8, MW=44.05 g/mol). It is commonly used in chemical manufacturing of polymers and glycols. It is also used to sterilize medical equipment (e.g. pacemakers, surgical kits) that cannot be exposed to heat or humidity. Due to its reactivity, ethylene oxide is a carcinogen. The United States Environmental Protection Agency (EPA), through its Integrated Risk Information System (IRIS), has set an inhalation unit risk (IUR) for EtO at 3.0×10^{-3} per µg/m^3 (5.5×10^{-3} per ppb), for adult increased cancer risk based on human data (US EPA, 2016). The IUR is an upper-bound estimate of excess cancer risk from continuous

Deleted: cell

Deleted: hydrocarbon

exposure to a compound at 1 μg/m^3 in air (US EPA, 2022b). An IUR for EtO of 3.0 × 10^{-3} per μg/m^3 implies that 3 excess cancer cases are expected to develop in 1000 people if exposed to 1 μg/m^3 (0.55 ppb) of EtO over a lifetime. Other risk estimates for different populations are included in the source EPA material (US EPA, 2016). Workplace limits for 8-hour and acute 5-min exposures are several orders of magnitude higher, on the order of 1 – 5 ppm (OSHA, 2002). The toxicity of this chemical makes accurate, high precision measurements of ambient and near-source concentrations imperative; this advance is described herein.

Formatted: Superscript

Formatted: Superscript

Background levels of EtO are challenging to measure via extractive methods such as canister sampling. EtO can be formed during storage in the canisters used (Hoisington and Herrington, 2021; US EPA, 2019; Hasegawa, 2001). The levels of reported EtO formation are on the order of hundreds of ppt. Hoisington and Herrington (2021) note EtO formation in blanks filled with humidified air but not dry air or inert gas, and thus hypothesize the reaction to be between larger hydrocarbons and oxygen, catalyzed by the presence of water and metal surfaces. Both canister type/coating (US EPA, 2019) and canister cleanliness/cleaning protocol (Hoisington and Herrington, 2021) are thought to impact EtO formation.

Reported background concentrations of EtO at select US National Air Toxics Trends monitoring sites (NATTS) for the Oct 2018 – March 2019 period average 0.297 μg m^{-3} and range between 0.185 – 0.397 μg m^{-3} (103 to 220 ppt) (US EPA, 2019). More recent EPA data from 2022 at Massachusetts measurement sites show 24-hour concentrations between 0 and 0.270 μg m^{-3} (0 – 150 ppt) (US EPA, 2022a) (data accessed 2022/8/30). Olaguer et al. (2020) report near-source 24 hr average concentrations in the 0.42 – 76.0 μg m^{-3} range (233 ppt – 42.2 ppb), the lower value representative of ambient background, and the higher value sampled near a vent at a sterilization facility. These measurements all rely on canister sampling methods. To date, this study is the first in-situ measurement of real EtO sources in the published literature.

Several additional in-situ instruments for the detection of EtO have been developed recently. Gupta et al. (2022) describe a cavity-enhanced absorption spectrometry method with precision < 1 ppb (1 sigma, 60 seconds) and 0.5 ppb (1 sigma, 15 minutes). Picarro, Inc. (2021) has publicized cavity ringdown spectroscopy (CRDS) instruments with detection limits of 0.1 – 0.25 ppb (3 sigma, 300 seconds) depending on instrument model. Entanglement Technologies (2022) lists a CRDS instrument with EtO detection at the ppb-level in 5 seconds with other VOCs detected, and at the ppt-level in 15 minutes in "lab-scan" mode. Aeris Technologies (2022) describes a laser-based EtO with 0.5 ppb sensitivity (1 sigma, 1 second). Here, we describe a commercially available Aerodyne EtO monitor (Aerodyne Research Inc., 2022b) based on direct-absorption spectroscopy that is capable of < 0.075 ppb precision at 1-second (1 sigma) and 0.020 ppb precision at 100 seconds (1 sigma). With frequent zeroing and data averaging we demonstrate a precision of < 4 ppt (1 sigma, 1 hr). Instrument performance and calibration is described. A months-long ambient EtO record at a site in Billerica, Massachusetts, USA is described, and enhancements are traced back to a potential inventory EtO source. This source, and another are confirmed via near-field mobile measurements.

2 Experimental

2.2 Instrument Description

The basis of our EtO monitor is our commercially available dual-laser tunable infrared direct absorption spectrometer (TILDAS-FD) platform (Aerodyne Research Inc., 2022a), which in this case is equipped with a single mid-infrared interband-cascade laser (nanoplus GmbH). For the system described herein, we use a multipass cell with 413 m optical pathlength and an active volume of 1.8 liters for continuous flow applications. The sample pressure was maintained between 20 Torr (26 mbar) and 30 Torr (40 mbar) throughout the experiments described in this paper. Details of the optical setup and flow system are described in the SI.

We measure EtO in a narrow wavelength window near 3065 cm^{-1} (3.26 µm), Figure 1. This figure fits an ambient spectrum divided by a scrubber-zeroed spectrum, such that all species except for EtO are near-zero (see Section 2.3). In total, more than 250 individual absorption lines from 6 molecular absorbers are included in the spectroscopic fit: EtO (114 lines), water (H_2O, 18 lines), formaldehyde (HCHO, 23 lines), ethane (C_2H_6, 28 lines), methane (CH_4, 12 lines), ethylene (C_2H_4, 56 lines). Methanol can be included in the fit optionally (32 lines). Centre wavelengths, linestrengths, and broadening coefficients of all molecules except EtO, ethane and methanol are from the HITRAN database (Gordon et al., 2017). Ethane and methanol lines are based on experiments by Harrison et al. (2012). The high-resolution line parameters for EtO at 3065 cm^{-1} were derived at Aerodyne. Initial knowledge of absorption at this wavelength was gained from high-resolution Fourier transform spectra by Lafferty et al. (2013).

2.3 Calibration and Zeroing

The EtO measurement is based on a set of experimentally acquired absorption lines. These experiments were done on a prototype TILDAS instrument with 76 m pathlength absorption cell, operating at 30 Torr. The absorption linestrengths were calibrated in February 2020 using a certified EtO standard (Apel Riemer, certified value 0.1023 ppm, August 2019) determined by P. Kariher at the US EPA to show good relative agreement (within 7%) among 18 tanks from 5 vendors (Kariher, 2022). Pressure-dependent EtO line broadening and other changes in instrument setup such as the inlet may lead to additional uncertainty or bias when operating the 413 m instrument at 20 Torr, and so additional calibrations are done regularly for this instrument.

Calibrations are performed by quantitative dilution of high-concentration EtO standards, to achieve a multi-point calibration curve (see SI, Figure S1). We find dry calibrations prone to long time constants, which we tentatively attribute to surface effects. Humid standard additions are preferred, as they most closely resemble sampling conditions.

We use a 2021 Airgas calibration standard, containing EtO (1.092 ppm ± 5%) and ethane (1.075 ppm ± 5%) in a balance of nitrogen (see SI, Figure S2). The inclusion of ethane in the calibration tank provides a secondary known species measurable by the instrument and not prone to reactivity or inlet effects. The average calibration factor for a set of standard addition calibrations performed over a representative week-long period is m = 0.981 ± 0.045 (95% error bars). This calibration factor

Deleted: Figure 1Figure 1

Deleted: across

Deleted: A measured spectrum at high-concentrations of EtO is shown in the SI, Figure S1.

Deleted: Methanol lines are based on experiments by Harrison et al. (2012).

Deleted: S2

Deleted: 075

Deleted: 092

Deleted: S3

implies 1 ppb of measured EtO would be corrected to 1.02 ppb EtO. However, we do not apply this small 2% correction to the data, given a certified tank uncertainty of 5% and the 4.6% error bars on the average calibration factor.

Uncertainties in the certified values of commercially available calibration tanks is of concern for accurate calibration of this and other EtO methods. A total of 4 commercially available standards have been measured by the TILDAS-FD-EtO monitor described here, varying in vendors, and at nominal concentrations of 1 ppm except where noted. Their retrieved concentrations deviated from their certified values by -2% (the above EtO and ethane standard), +9%, -417% (standard at 0.5 ppm) and +18%.

Spectral backgrounding (or autobackgrounding) is done by intermittently and regularly measuring air free of EtO. Each acquired background spectrum is used to divide sample spectra for the subsequent period, reducing the impact of drift due to instrumental effects like optical fringes and spectral baseline effects. The use of scrubbed air provides a near-humidity match between sample and background spectra, effectively flattening out the curvature of the baseline present under the EtO lines due to strong neighboring water absorptions. We have not extensively tested whether the scrubber decreases the other species measured in the fit (HCHO, C_2H_6, C_2H_4, CH_4, etc.), but they appear in the divided ambient spectra with near-zero concentrations (Figure 1). For species with significant ambient backgrounds like CH_4, this indicates that the scrubber is non-destructive to CH_4. Laboratory experiments suggest scrubber EtO breakthrough on the scale of 3% is possible (3-5 SLPM flow rates) at high mixing ratios (hundreds of ppb). Indeed, mobile near-source measurements have shown such EtO breakthrough when an autobackground occurs within a high-concentration plume. Correction of this data is possible after-the-fact by manually offsetting baselines or performing a spectral refit of the data.

The frequency of autobackgrounds is chosen to match the sampling strategy. Mobile measurements aimed at capturing plumes (enhancements over background lasting typically 1-3 minutes) use a 5- to 15-minute autobackground cycle. This is a practical decision that reduces the chance of a zero interfering with a plume during a downwind transect of a facility, and is defensible as we typically are less concerned with time averaging and ppt-level baseline drift during near-source measurements. Stationary sampling of background concentrations, on the other hand, yields best long-term averaging with a 2-minute cycle

3 Results

3.1 Instrument Performance

Precision for the TILDAS-FD EtO monitor at 1-second are < 70 ppt (1-sigma), regardless of stationary or mobile measurements.

Figure 2 compares stationary and mobile ambient measurement Allan-Werle variance plots (Werle, 2011). Blue traces show stationary performance, with best precisions achieved when stationary by altering humidity-matched zeroes with ambient measurements every 2 minutes for a 50% duty cycle. The precision improves with averaging time, from a base precision of 44 ppt (1-sigma at 2-sec) reaching 13 ppt at 2-minutes, 6.0 ppt at 15 minutes and 4.1 ppt at 1 hour (all precisions at 1-sigma).

The TILDAS-EtO monitor has also been used for near-source mobile monitoring, with less frequent autobackgrounds (5- to 10-minute frequencies). The instrument shows sensitivity to truck motion, particularly quick turns or stops which manifest as

Deleted: The
Deleted: subsequent
Formatted: Subscript
Formatted: Subscript
Deleted: Figure 1
Deleted: :
Deleted: mobile
Deleted: brief
Deleted: to
Deleted: interfer
Deleted: ence
Deleted: transects; s
Deleted: uses
Deleted: - to 5
Deleted: to optimize long-term averaging
Deleted: Figure 2Figure 2
Deleted: Measurements average down well

negative deviations in mixing ratio on the order of 0.5 ppb. Optimizing optical alignment minimizes but does not eliminate these effects, which are largely attributed to strain on the laser focusing objective. Continuous vibrations do not manifest as negative deviations, instead impacting the overall noise. Performance while in motion on the highway is shown in Figure 2 (red traces). For these measurements, the instrument was mounted in the Aerodyne Mobile Laboratory in a vibration-isolated rack and operated with a 10-minute humidity-matched zeroing cycle. The 1-second precision of 50 ppt averages to 28 ppt in 2 minutes.

3.2 Ambient Measurements

A months-long record of ambient EtO in Billerica, Massachusetts, USA was acquired (Figure 3), spanning winter, spring, and summer 2022. Averaging the hourly data for the entire period (with standard deviation in parentheses) yields Avg (SD) = 18 (22) ppt. The standard deviations given reflect the combination of instrument noise as described above and the variability of EtO in ambient air. Histograms comparing winter and summer concentraitions are shown in Figure S3. Hourly averages for summertime data are less noisy than wintertime data due to the more aggressive zeroing cycle (2 mins vs 30 mins). Summertime concentrations (1 July – 4 Aug) of 33 (13) ppt appear slightly elevated compared to winter averages (9 Feb – 30 April) 12 (23) ppt measurements. We exclude the intermediate spring data (May) from these averages. The averages are different at the 95% confidence level using Gaussian statistics and standard error of the mean (see SI, Table S3). These data are consistent with recent data reported by the EPA for 4 Massachusetts sites (US EPA, 2022a): 2022 observations accessed 8/20/2022 range between 0 and 0.270 μg m^{-3} (0 – 150 ppt) with a median of 0.090 μg m^{-3} (50 ppt); they are below 2019 levels shown for EPA NAATS sites in New York and Pennsylvania (US EPA, 2019) of 0.298 – 0.361 μg m^{-3} (165 – 201 ppt), though the EPA has since noted that true background concentrations are unknown due to the influence of canister artifacts (US EPA, 2021).

Several distinct EtO enhancement events are evident in the ambient record. One such event on 3/27/2022 is shown in Figure 4. This figure shows two plumes, the larger of the two reaching concentrations of 500 ppt, and lasting 3-4 hours near midnight local time. No EtO activity (e.g., calibrations) was occurring in the lab during this week. During these winter and spring roof-top measurements, the EtO monitor briefly switches to laboratory air prior to humidity-matched autobackgrounds, providing several seconds of indoor air sampling. The laboratory air shows an "echo" of the outdoor EtO event ~3 hours delayed, and slightly broadened, with a maximum concentration of 168 ppt, which we attribute to the building's ventilation system gradually mixing in outdoor air. This observation highlights the fact that indoor air quality is directly impacted by outdoor EtO concentrations.

Back-trajectory simulations for this event were performed using NOAA's HYSPLIT model (Rolph et al., 2017; Stein et al., 2015) (see Figures S4 – S5). These simulations suggest that regional transport was from the south-west during this time. This trajectory passes over a commercial sterilization facility approximately 35 km away that is known by the EPA to use EtO (US EPA, 2022c). In the following section, we describe near-field mobile measurements of this source showing clear EtO enhancements downwind. These ambient measurements highlight the benefits of the high-precision TILDAS-FD-EtO sensor

Deleted: Optical
Deleted: are
Deleted: less impactful
Deleted: Figure 2Figure 2
Deleted: and spring
Deleted:
Deleted: Figure 4Figure 4
Deleted: engine
Deleted: S5
Deleted: S6

over alternative methods like canister sampling, which typically have long integration times (24 hours) that would wash out brief events and are prone to sampling artifacts at 100's of ppt levels (US EPA, 2021; Hoisington and Herrington, 2021).

3.3 Near-Field Mobile Measurements

Motivated by the sporadic enhancement events in the ambient measurement record, mobile measurements of two commercial sterilization facilities in Massachusetts (US EPA, 2022c) were conducted in August 2022. The first source visited, "Facility A", was the facility identified through Hysplit trajectory explorations of the 3/27/2022 event. Facility A was visited over the course of ~4 hours, split between morning and afternoon. Average downwind concentrations are summarized in Figure 5, showing clear enhancements above background downwind of the facility. Concentration enhancements ~600 m from the source were around 5 ppb, with enhancements as high as 300 ppb measured 35 m from the facility. Additional transects, time series and spatial averages are shown in the SI.

The second source measured, "Facility B", is also a commercial sterilization facility (US EPA, 2022c), and is located 15 km miles south of the Billerica MA stationary measurement site. The EPA has conducted a risk assessment of this facility and found enhanced cancer risk (US EPA, 2022c). Facility B also showed enhancements above background on this measurement day (maximum of 7.5 ppb 60 m downwind), though at far lesser concentrations than Facility A. Further details are presented in the SI.

Deleted: Figure 5Figure 5

4 Conclusions

The TILDAS-FD-EtO monitor achieves precisions of <75 ppt or <0.075 ppb in 1 second and < 20 ppt in 100 seconds (1-sigma precisions), with averaging down to 4 ppt in an hour (1-sigma) when operated with frequent humidity-matched zeroes. Ambient measurements at a Massachusetts site reveal EtO concentrations on the order of 18 ppt (22 ppt standard deviation). Distinct EtO events lasting a few hours are observed in the ambient record, with back trajectory simulations suggesting an EtO source nearly 35 km away. Mobile measurements directly downwind of this medical sterilization facility, as well as another sterilization facility in the state, confirm the presence of EtO emissions at both sites, with downwind concentrations in the 0.5 ppb to 700 ppb range depending on source identity and distance downwind. These measurements highlight how continuous in-situ EtO monitoring with a high-precision sensor can provide information leading directly to EtO point source identification.

Data availability

Ambient ethylene oxide dry air mixing ratios, hourly averages and mobile measurement data is publicly and freely available at https://osf.io/jeywd/?view_only=421c0d48e2d1449488c14f883a7859b6

Author Contribution

The manuscript was written through contributions of all authors.

Competing Interests

The authors declare no competing interests.

Disclaimer

The US Environmental Protection Agency funded this instrument development, but no formal review of these results has been conducted. This work has not been reviewed by US EPA. The views and conclusions expressed are strictly based on the evaluation of Aerodyne Research, Inc. scientists only.

Acknowledgements

Development of the TILDAS-FD-EtO instrument with 413 m cell was funded by the US Environmental Protection Agency under SBIR award number 68HERC21C0047. The authors thank Jean-Marie Flaud and colleagues (Lafferty et al., 2013) for insights into high resolution Fourier transform infrared spectra for EtO.

References

Aeris Technologies: MIRA Pico EtO - ultrasensitive ethylene oxide analyzer, 2022. https://aerissensors.com/wp-content/uploads/2019/12/MIRA-Pico_EtO_191208_FINAL_quartz.pdf, last access: 2022-09-28.

Aerodyne Research Inc.: Laser trace gas and isotope analyzers, 2022a. https://www.aerodyne.com/product/laser-trace-gas-and-isotope-analyzers/, last access: 2022-09-28.

Aerodyne Research Inc.: TILDAS compact single laser ethylene oxide analyzer, 2022b. https://www.aerodyne.com/wp-content/uploads/2022/01/EthyleneOxide.pdf, last access: 2022-09-28.

Entanglement Tech: AROMA-ETO precision chemical vapor analyzer, 2022. https://entanglementtech.com/wp-content/uploads/2021/10/AROMA-ETO-Specifications.pdf, last access: 2022-10-6.

Gordon, I. E., Rothman, L. S., Hill, C., Kochanov, R. V., Tan, Y., Bernath, P. F., Birk, M., Boudon, V., Campargue, A., Chance, K. V., Drouin, B. J., Flaud, J. M., Gamache, R. R., Hodges, J. T., Jacquemart, D., Perevalov, V. I., Perrin, A., Shine, K. P., Smith, M. A. H., Tennyson, J., Toon, G. C., Tran, H., Tyuterev, V. G., Barbe, A., Császár, A. G., Devi, V. M., Furtenbacher, T., Harrison, J. J., Hartmann, J. M., Jolly, A., Johnson, T. J., Karman, T., Kleiner, I., Kyuberis, A. A., Loos, J., Lyulin, O. M., Massie, S. T., Mikhailenko, S. N., Moazzen-Ahmadi, N., Müller, H. S. P.,

Naumenko, O. V., Nikitin, A. V., Polyansky, O. L., Rey, M., Rotger, M., Sharpe, S. W., Sung, K., Starikova, E., Tashkun, S. A., Auwera, J. V., Wagner, G., Wilzewski, J., Wcisło, P., Yu, S., and Zak, E. J.: The hitran2016 molecular spectroscopic database, Journal of Quantitative Spectroscopy and Radiative Transfer, 203, 3-69, https://doi.org/10.1016/j.jqsrt.2017.06.038, 2017.

Gupta, M., Chan, A. P., Sullivan, M. N., and Gupta, R. M.: Trace measurements of ethylene oxide using cavity-enhanced absorption spectrometry near 3066 cm–1, Aerosol Air Qual. Res., 22, 220046, https://dx.doi.org/10.4209/aaqr.220046, 2022.

Harrison, J. J., Allen, N. D. C., and Bernath, P. F.: Infrared absorption cross sections for methanol, Journal of Quantitative Spectroscopy and Radiative Transfer, 113, 2189-2196, http://dx.doi.org/10.1016/j.jqsrt.2012.07.021, 2012.

Hasegawa, A.: Measurement of ethylene oxide in the atmosphere, J. Environ. Chem., 11, 11-15, 2001.

Hoisington, J. and Herrington, J. S.: Rapid determination of ethylene oxide and 75 VOCs in ambient air with canister sampling and associated growth issues, Separations, 8, 35, https://doi.org/10.3390/separations8030035, 2021.

Kariher, P.: Status of EtO source measurements, 2022 National Ambient Air Monitoring Conference, Pittsburgh, PA, 2022-08-222022.

Lafferty, W. J., Flaud, J. M., Kwabia Tchana, F., and Fernandez, J. M.: Raman and infrared spectra of the ν1 band of oxirane, Mol. Phys., 111, 1983-1986, https://dx.doi.org/10.1080/00268976.2013.775516, 2013.

Olaguer, E. P., Robinson, A., Kilmer, S., Haywood, J., and Lehner, D.: Ethylene oxide exposure attribution and emissions quantification based on ambient air measurements near a sterilization facility, Int. J. Environ. Res. Public Health, 17, 42, https://dx.doi.org/10.3390/ijerph17010042, 2020.

OSHA: Ethylene oxide fact sheet, 2002. https://www.osha.gov/sites/default/files/publications/ethylene-oxide-factsheet.pdf, last access: 2021-09-28.

Picarro Inc.: Ambient air monitoring system for ethylene oxide, 2021. https://www.picarro.com/products/ambient_air_monitoring_system_for_ethylene_oxide, last access: 2021-09-28.

Rolph, G., Stein, A., and Stunder, B.: Real-time environmental applications and display system: Ready, Environ. Model. Softw., 95, 210-228, https://doi.org/10.1016/j.envsoft.2017.06.025, 2017.

Stein, A. F., Draxler, R. R., Rolph, G. D., Stunder, B. J. B., Cohen, M. D., and Ngan, F.: NOAA's HYSPLIT atmospheric transport and dispersion modeling system, Bull. Amer. Meteor., 96, 2059-2077, https://doi.org/10.1175/bams-d-14-00110.1, 2015.

US EPA: Evaluation of the inhalation carcinogenicity of ethylene oxide, National Center for Environmental Assessment Office of Research and Development, U.S. Environmental Protection Agency, Washington DC, Report EPA/635/R-16/350Fc, 2016. https://iris.epa.gov/static/pdfs/1025_summary.pdf, last access: 2022-09-28.

US EPA: IRIS assessments: Ethylene oxide, 2017. https://cfpub.epa.gov/ncea/iris2/chemicalLanding.cfm?substance_nmbr=1025, last access: 2022-09-28.

US EPA: Ethylene oxide data summary from national air toxics trends stations and urban air toxics monitoring program sites, 2019. https://www.epa.gov/hazardous-air-pollutants-ethylene-oxide/ethylene-oxide-data-summary-national-air-toxics-trends, last access: 2022-08-29.

US EPA: EPA's work to understand background levels of ethylene oxide, 2021. https://www.epa.gov/hazardous-air-pollutants-ethylene-oxide/epas-work-understand-background-levels-ethylene-oxide, last access: 2022/8/30.

US EPA: Monitor values report - hazardous air pollutants, 2022a. https://www.epa.gov/outdoor-air-quality-data/monitor-values-report-hazardous-air-pollutants, last access: 2022/8/30.

US EPA: Integrated risk information system (IRIS) glossary, 2022b. https://iaspub.epa.gov/sor_internet/registry/termreg/searchandretrieve/glossariesandkeywordlists/search.do?details=&vocabName=IRIS%20Glossary, last

US EPA: Ethylene oxide commercial sterilization facilities, 2022c. https://www.epa.gov/hazardous-air-pollutants-ethylene-oxide/ethylene-oxide-commercial-sterilization-facilities, last access: 2022/08/30.

Werle, P.: Accuracy and precision of laser spectrometers for trace gas sensing in the presence of optical fringes and atmospheric turbulence, Applied Physics B, 102, 313-329, 10.1007/s00340-010-4165-9, 2011.

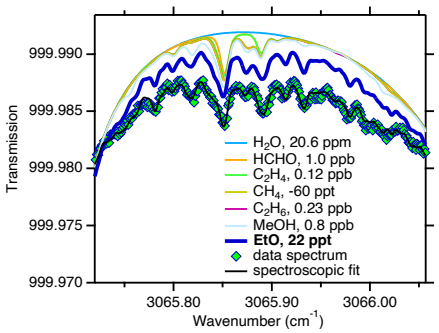

Figure 1. Spectrum of EtO and other gaseous absorbers in the spectral window that are included in the spectroscopic fit. A measured spectrum (green diamonds, 24 hr average ambient spectrum, humidity-matched scrubber zeroes) is shown overlaid with the final fit (black trace). Individual fit components include water (H_2O), formaldehyde (HCHO), ethylene (C_2H_4), methane (CH_4), ethane (C_2H_6) and methanol (MeOH). This figure fits an ambient spectrum divided by a scrubber-zeroed spectrum, such that all species except for EtO are near-zero (see Section 2.3).

Formatted: English (UK)

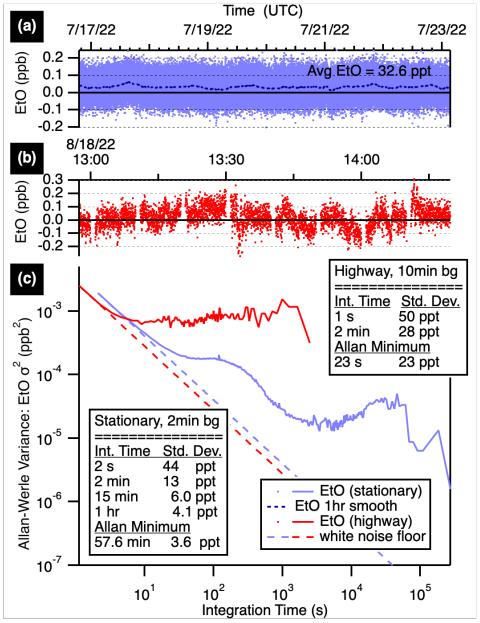

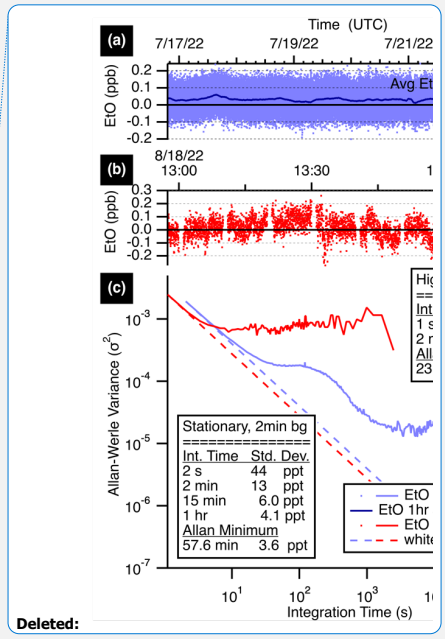

Deleted:

Figure 2. Time series (a, b) and Allan-Werle variance plots (c) showing EtO precisions at various averaging times while stationary with 2-min autobackgrounds (blue), and while mobile on the highway with 10-min backgrounds (red). The stationary data (a) averages to 32.6 ppt EtO, with a 1-hour smooth (dotted line) shown.

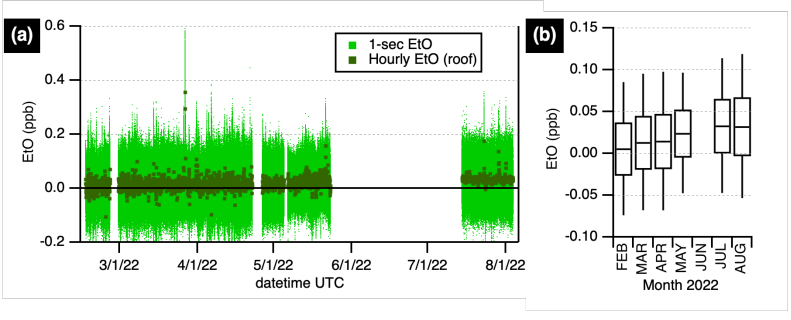

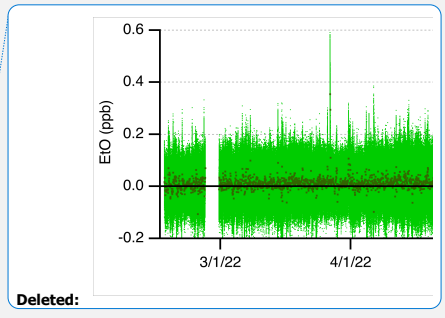

Deleted:

Figure 3. Ambient ethylene oxide at a site in Billerica, Massachusetts, USA. Panel (a): Data at 1-second (pale green) is shown alongside hourly averages (dark green squares). Panel (b): Monthly box plot showing the median, 25th and 75th quartiles, with whiskers extending to the 5th and 95th percentiles. Data prior to 6/2022 were acquired from a roof-top inlet with humidity-matched autobackgrounds every 30 minutes; data after 7/2022 were acquired from a 3-meter inlet with humidity-matched autobackgrounds every 2 minutes. Gaps in the time series are due to laboratory or field experiments.

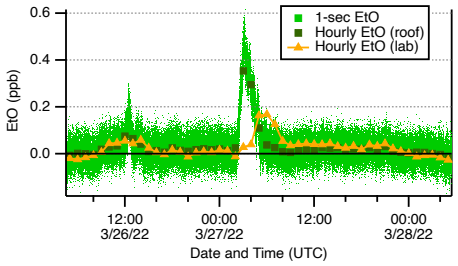

Figure 4. Ethylene oxide events measured on the roof-top inlet. Outdoor data at 1-second data (pale green) is shown alongside hourly averages (dark green squares) averages. Laboratory air sampled prior to autobackgrounds (orange triangles) is shown.

Formatted: Superscript
Formatted: Superscript
Deleted: was
Deleted: 5
Deleted: was

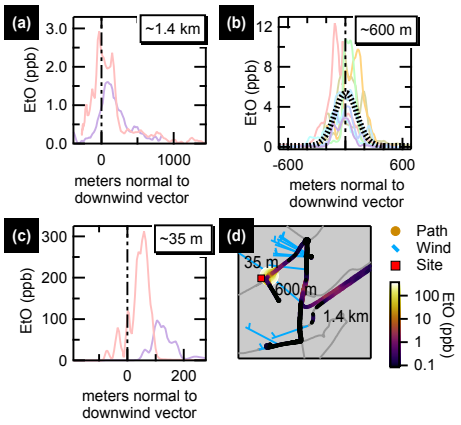

Figure 5. Summary of transects downwind of Facility A. Transects are plotted normal to the wind vector for paths driven along 3 roads approximately 35 m (a), 600 m (b) and 1.4 km (c) downwind of Facility A. The average of 600 m transects (black dotted line) is shown for Panel B. A map (d) shows the facility location (red square) with the three main transect roads labelled by distance downwind. The driven path is colored and sized by EtO concentration. Wind barbs (blue) are tethered to the truck path, with feather end of the staff pointing into the wind.

Formatted: Keep with next

Deleted: vectors

Deleted: point into the wind

Response to Reviewer Comments for

"Ethylene Oxide Monitor with Part-per-Trillion Precision for In-Situ Measurements"

by Yacovitch et al.

Reviewer comments are shown in blue, and responses are shown in black. **Bolded** text indicates text that has changed.

Reviewer comments "RC1"

https://doi.org/10.5194/amt-2022-294-RC1

This paper describes an instrument and associated measurement and data processing protocols for measurements of the important carcinogen trace gas ethylene oxide. As discussed, these measurements are extremely challenging due to the very low ambient concentrations at pptv levels and a number of potential spectroscopic interferences from higher concentration ambient constituents. This paper is highly relevant, the discussion is clearly written, and the measurements are carefully carried out. The ambient ethylene oxide enhancements downwind of two facilities known for operations involving this gas provide clear convincing evidence for the merits of this instrument as well as the instrument performance in real-world ambient conditions. This reviewer recommends final publication of this paper after the authors consider the following minor comments/suggestions to improve the paper quality further.

We thank the reviewer for their in-depth read and useful comments. We address them all below:

1. Would be informative to briefly describe the definition for the inhalation unit risk discussed in the Introduction.

We elaborate as follows:

The United States Environmental Protection Agency (EPA), through its Integrated Risk Information System (IRIS), has set an inhalation unit risk **(IUR)** for EtO at 3.0×10^{-3} per µg/m^3 (5.5×10^{-3} per ppb), for adult increased cancer risk based on human data (US EPA, 2016). **The IUR is an upper-bound estimate of excess cancer risk from continuous exposure to a compound at 1 µg/m^3 in air (US EPA, 2022b). An IUR for EtO of 3.0×10^{-3} per µg/m^3 implies that 3 excess cancer cases are expected to develop in 1000 people if exposed to 1 µg/m^3 (0.55 ppb) of EtO over a lifetime. Other risk estimates for different populations are included in the source EPA material (US EPA, 2016).**

2. Would also be informative to briefly describe in the Introduction that ethylene oxide (C_2H_4O, MW = 44.052 g/mole) is a cyclic three-membered ring structure with the O atom connected to both carbons.

"Ethylene oxide (EtO, also known as EO or oxirane) is a reactive **compound with a strained 3-member ether ring (C_2H_4O, CAS# 75-21-8, MW=44.05 g/mol)."**

3. The discussion of the simulations in Fig. 1 should be modified to indicate that you employed the Harrison et al. line parameters also for ethane here. The conditions of temperature and pressure should be included in figure caption. I am a little confused by the choice for the simulated concentrations included in Fig. 1. Shouldn't ambient levels of CH_4 around 2 ppm and H_2O levels of 1 to 4% be used in these simulations or do these simulations represent the residual concentrations after subtracting the humidified matched background spectra? This should be discussed here.

We add the ethane line source, and move this statement directly after the HITRAN mention:

"[…] all molecules except EtO, **ethane** and methanol are from the HITRAN database (Gordon et al., 2017). **Ethane and methanol lines are based on experiments by Harrison et al. (2012).**"

Yes, the spectrum is a "zeroed" ambient spectrum, so ambient levels of CH_4, ethane and H_2O are divided out of the fit. We explain in a few places:

Upon first mention of Figure 1:

"[…] Figure 1. **This figure fits an ambient spectrum divided by a scrubber-zeroed spectrum, such that all species except for EtO are near-zero (see Section 2.3)."**

In the Figure 1 caption:

" Figure 1. Spectrum of EtO and other gaseous absorbers in the spectral window that are included in the spectroscopic fit. A measured spectrum (green diamonds, 24 hr average ambient spectrum, humidity-matched **scrubber** zeroes) is shown overlaid with the final fit (black trace). Individual fit components include water (H_2O), formaldehyde (HCHO), ethylene (C_2H_4), methane (CH_4), ethane (C_2H_6) and methanol (MeOH). **This figure fits an ambient spectrum divided by a scrubber-zeroed spectrum, such that all species except for EtO are near-zero (see Section 2.3)."**

In Section 2.3:

The use of scrubbed air provides a near-humidity match between sample and background spectra, effectively flattening out the curvature of the baseline present under the EtO lines due to strong neighboring water absorptions. **We have not extensively tested whether the scrubber decreases the other species measured in the fit (HCHO, C_2H_6, C_2H_4, CH_4, etc.), but they appear in the divided ambient spectra with near-zero concentrations (Figure 1). For species with significant ambient backgrounds like CH_4, this is indicates that the scrubber is non-destructive to CH_4.**

4. The meaning of normalized in Fig. S1 should be included in the figure caption just as you did in the Supplement text on line 46. Also the spelling of "Mcmanus" on line 27 in the Supplement should be corrected to "McManus". Also maybe indicate why you get a normalized value up to 1.04 in Fig. S1. Is this due to noise or small inaccuracies in your polynomial baseline fitting here?

The capitalization of "McManus" has been corrected.

We have added a short discussion of this figure and moved it in the SI under the "S4.1 Facility A" header, since it is not meant to illustrate the 0-1 transmission normalization procedure described in the SI section "S1.1 Optical setup […]" section

The archived spectra can be used to unambiguously spectrally fingerprint the EtO observed at these facilities. For example, Figure S10 (top) shows raw measured signal out of plume (black) overlaid on signal in-plume (gold area) at Facility A. In Figure S10 (bottom), we manually divide the in-plume and out-of-plume spectra to reveal the spectral signature of EtO. Line scars at the positions of the water lines are observable (green spikes) due to slight variations in laser peak position. The blue line is a transmission simulation of EtO only, and clearly matches the experimental result.

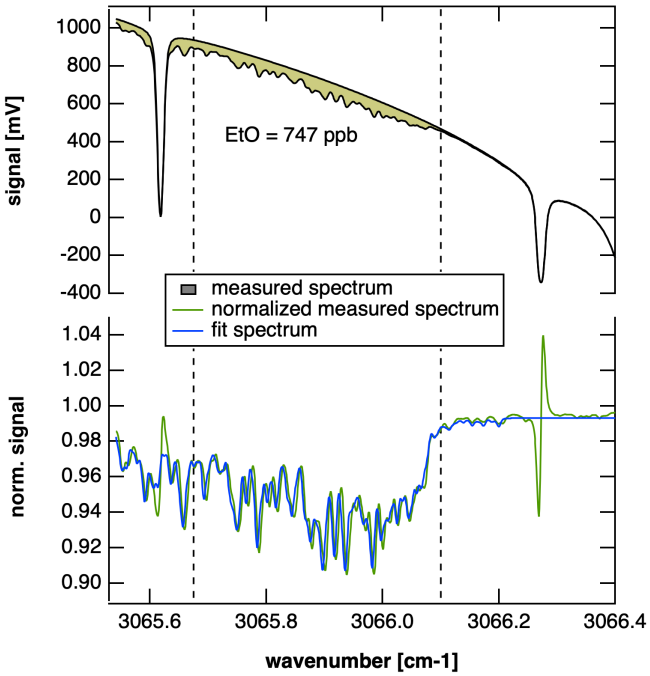

Figure S10. Summary spectra comparing instantaneous Facility A measurement of 747 ppb (in-plume, gold) to an out-of plume spectrum. The top shows signal as a function of wavenumber, with EtO contributions highlighted in yellow. The bottom shows a divided spectra in-plume/out-of-plume (green) and transmission simulation of EtO only.

5. Indicate in the figure caption of Fig. S1 if the blue fit spectrum includes all the gases in the inset of Fig. 1?

It does not. See discussion above

6. The certified concentrations for EtO (1.075 ppm) and ethane (1.092 ppm) on line 76 needs to be reversed in accordance with the Analytical Results of Fig. S3. Also the X-

axis labels in Fig. S2 in both cases needs to be corrected to 1.092 ppm in accordance with the Analytical Results. Also, please explain in Fig. S2 why you label the left hand plot "Dry Calibration" as the H_2O values here are actually larger than the right hand plot.

We have corrected this concentration typo in the text. We have confirmed that the correct tank concentrations were used in the calibration workups, including those shown in Fig S2. The axis Labels for Fig S2 have been corrected to read 1.092.

The water concentrations were in scientific notation, and hard to parse (6E4 ppb for the dry calibration; 1.5E7 ppb for the standard addition). We have changed both to percent water (0.006% for the dry calibration vs 1.5% for the standard addition) for clarity.

7. On line 60 in the Supplement, you should consider either adding what is in the scrubber cartridge that removes EtO and not H_2O or indicate this is proprietary.

We add the following to the SI:

For humidity-matched zeroes, a parallel flow path is set up, with a length-matched piece of tubing and **6" by 1"** scrubber cartridge isolated by two solenoid valves. **We use a manganese dioxide/copper oxide catalyst as scrubber: Carulite 500® (Carus LLC), heated to 150 C.**

8. On line 87 in the discussion of dividing the subsequent sample spectra, it would be important to indicate if you employ the averaged background spectra over the ambient interval or do you use the updated background spectra for the subsequent ambient spectra? How much do these subsequent background spectra change (i.e., the difference of background spectra).

We alter the text to specify that we use the nearest prior background spectrum:

"**Each acquired** background spectrum is used to **divide sample spectra for the subsequent period,** […]"

We have analyzed a 24 hr period of data on 7/20/2022 with 2-minute backgrounds. The average background-to-background delta is 21 ppt. For reference, the average ambient EtO on this day was 29 ppt (sdev = 48 ppt).

Each background is a 10-second average. The collected raw background spectra, with their deep water lines, were each divided by the average 24hr background spectrum prior to refitting, so that the input spectra had similar characteristics (flattened baseline about the EtO lines) as the fit sample spectra. A spectral fit of these data then yields a measured "zero" EtO for each background.

The average background-to-background delta of 21 ppt is on the same scale as the expected instrument performance on the timescale of these backgrounds: the Figure 2 Allan-Werle variance plot shows a 10 sec 1σ precision of 20.8 ppt; and a 2 min 1σ precision of 13 ppt. This implies that for 7/20/2022, background-to-background drift is being optimally mitigated at a 2-min zero cycle, which can also be seen from the variance plot itself.

9. Line 90, what scrubber breakthough are you referring to, breakthrough in EtO or H_2O? The text implies EtO breakthrough, but this should be spelled out.

We clarify:

"Laboratory experiments suggest scrubber **EtO** breakthrough on the scale of 3% is possible (3-5 SLPM flow rates) at high mixing ratios (hundreds of ppb). Indeed, mobile near-source measurements have shown such **EtO** breakthrough […]"

10. Line 95 where you indicate the autobackground cycles, I am confused by the cycle values. Shouldn't the mobile measurements employ more frequent background measurements to capture the greater potential due to spatial changes in H_2O and the reverse for stationary samples? Please further explain.

The scrubber provides good but imperfect humidity matching, and so we continuously fit water in between zeroes. We have thus not found spatial changes in H_2O on the timescale of a mobile zero to be of concern. We rework this paragraph to further explain the basis for our zero timing:

"The frequency of autobackgrounds is chosen to match the sampling strategy**. Mobile** measurements aimed at capturing plumes (enhancements over background **lasting typically 1-3 minutes**) use a 5- to 15-minute autobackground cycle. **This is a practical decision that reduces the chance of a zero interfering with a plume during a downwind transect of a facility, and is defensible as we typically are less concerned with time averaging and ppt-level baseline drift during near-source measurements.** Stationary sampling of background concentrations, on the other hand, **yields best long-term averaging with a 2-minute cycle.**"

11. In Table S1 please indicate what * refers to in the Table next to the value 0.999

The original note indicated that the first dry calibration of the measurements was an outlier at 0.895 (low). We remove this asterisk, as the remaining calibrations are still within a week-long period.

12. In Fig. 2c, you should add to the Y-axis label the units ppb^2

The Y axis has been relabeled:

"**Allan-Werle Variance: EtO σ^2 (ppb^2)**"

13. Line 103: I would change the wording " Measurements average down well" to something like" The variance improves with averaging time....", which better describes the plot Fig. 2c.

We reword:

"**The precision improves with averaging time,** […]"

14. Line 107: You should reword " Optical alignment minimizes ..." to something like " Adjustments to optical alignment ...." Could small changes in the multipass highly dense spot pattern or resulting changes in optical cell noise also be a partially responsible?

The optical cell's mirrors are fixed in position and orientation, and so the spot pattern itself is very robust. An early exit of the laser beam from the cell is possible with very poor alignment of the input mirrors, but this is a dramatic effect, and not something that we have observed in motion. The main culprit is the focusing objective, as we describe in the text.

We further reword to:

"The instrument shows sensitivity to truck motion, particularly quick turns or stops which manifest as negative deviations in mixing ratio on the order of 0.5 ppb. **Optimizing optical** alignment minimizes but does not eliminate these effects, which are largely attributed to strain on the laser focusing objective."

15. In Fig. 2c, you should more clearly highlight in the plot the results for the EtO 1 hour smooth. As plotted, I have a hard time recognizing this 1 hour smooth. Are you referring to the portion of the variance between 10^3 to 10^5 sec? If so, you should darken this more in the plot.

The 1-hr smooth is for the stationary data due to the density of data shown. We have changed the line type and figure caption to clarify.

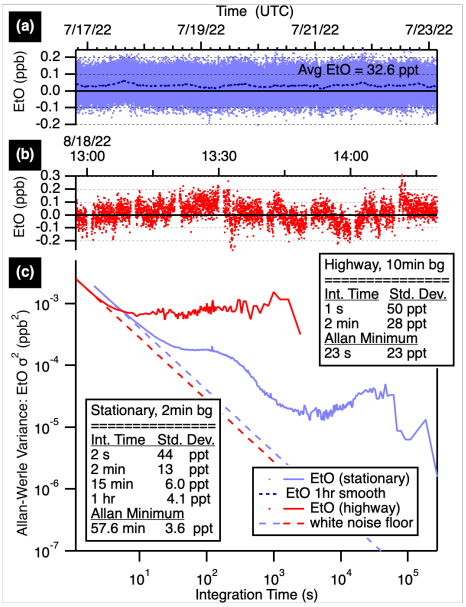

Figure 2. Time series (a, b) and Allan-Werle variance plots (c) showing EtO precisions at various averaging times while stationary with 2-min autobackgrounds (blue), and while mobile on the highway with 10-min backgrounds (red). **The stationary data (a) averages to 32.6 ppt EtO, with a 1-hour smooth (dotted line) shown.**

16. On Line 108: I would think about rewording the statement "Continuous vibrations are less impactful..", as the red in-motion variance clearly shows reduced performance relative to the blue stationary performance. I think you are referring to the very large negative 0.5 ppb instantaneous deviations and not the more sustained red variance. Maybe adding a caveat to your statement?

We rephrase: "Continuous vibrations **do not manifest as negative deviations, instead impacting the overall noise.**"

17. It would be useful to provide an additional Fig. 3b plot showing only the hourly measurements with an expanded scale from say -0.05 to +0.05 ppb. This would highlight better the two regimes. I just now saw this information is contained in your Fig. S4 and would leave it up to the co-authors to include a new Fig. 3b.

We reference Figure S3 (old Figure S4) in the text explicitly and add a panel to panel to Figure 3 showing a monthly box plot:

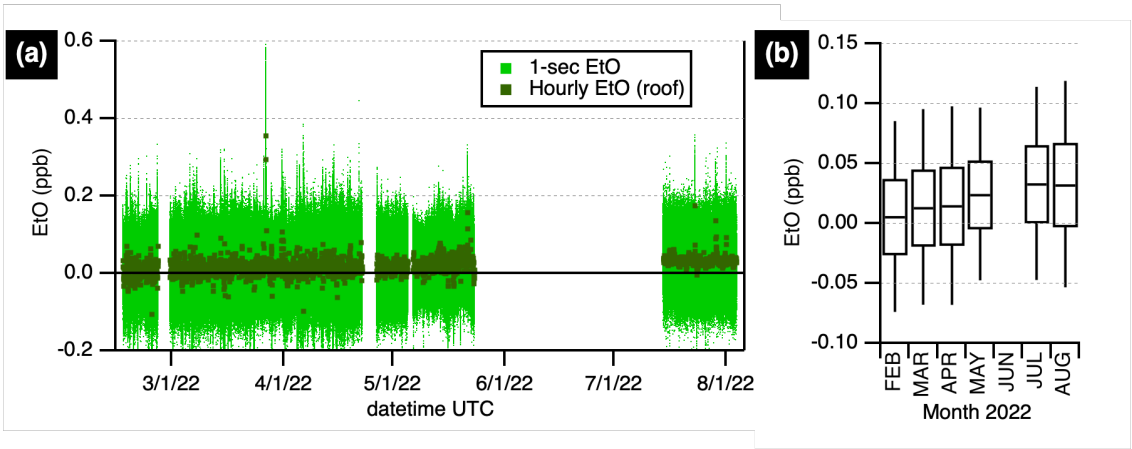

Figure 3. Ambient ethylene oxide at a site in Billerica, Massachusetts, USA. Panel (a): Data at 1-second (pale green) is shown alongside hourly averages (dark green squares). Panel (b): Monthly box plot showing the median, 25th and 75th quartiles, with whiskers extending to the 5th and 95th percentiles. Data prior to 6/2022 were acquired from a roof-top inlet with humidity-matched autobackgrounds every 30 minutes; data after 7/2022 were acquired from a 3-meter inlet with humidity-matched autobackgrounds every 2 minutes. Gaps in the time series are due to laboratory or field experiments.

18. Line 128: It would be important to point out the importance of your observations that indoor laboratory air echoes outside air offset by 3 hours to highlight that a typical building ventilation system only minimally removes EtO by a factor of 2.

"The laboratory air shows an "echo" of the outdoor EtO event ~3 hours delayed**, and slightly broadened, with a maximum concentration of 168 ppt**, which we attribute to the building's ventilation system gradually mixing in outdoor air. **This observation highlights the fact that indoor air quality is directly impacted by outdoor EtO concentrations.**"

19. The back trajectory in Fig. S6 provides very useful information but the Google Street View inset really doesn't add anything. I would recommend providing a more convincing view of this facility (if you can legally show a picture of this sterilization facility) or remove the inset.

We choose not to publish facility images, but have added a panel next to Figure S6 that shows the location of both potential EtO facilities referenced in US EPA, 2022b, along with the location of the rooftop measurements.

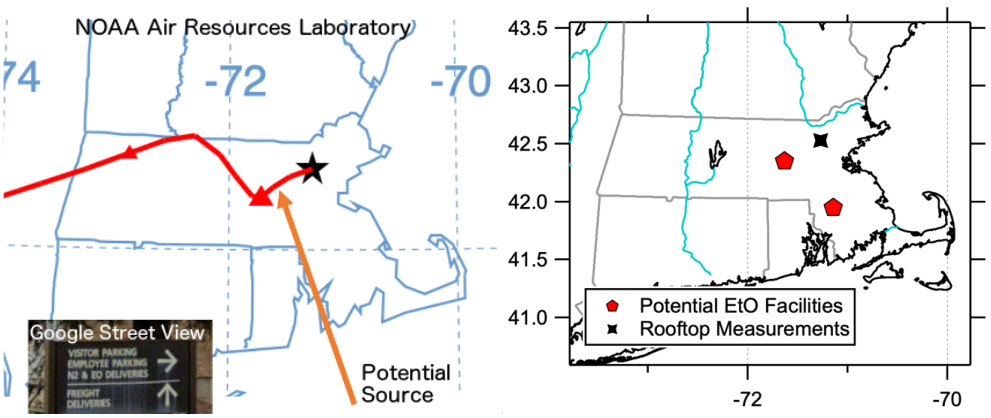

Figure S5. Left: Detail of back trajectory (NOAA Air Resources Laboratory). The orange arrow indicates location of one potential EtO source in the state. A roadside-view of this facility's signage is inset (© Google Street View), with "EO deliveries" noted. **Right: Location of rooftop measurements (black marker) and two potential EtO facilities (red markers) in the state of Massachusetts. Map outlines from NOAA (NOAA, 2013).**

20. In the Figures S4 showing facility A and the wind barbs, the facility A site indicator should be made larger in each case. Also the conventional definition of a wind barb indicates the direction from which the wind is blowing. The explanation in the caption of Fig. S7 and Fig. 5 indicating the wind barbs pointing into the wind is a little confusing given the conventional definition. This needs to be clarified.

Facility transect figures have had the facility markers enlarged, as in the example below.

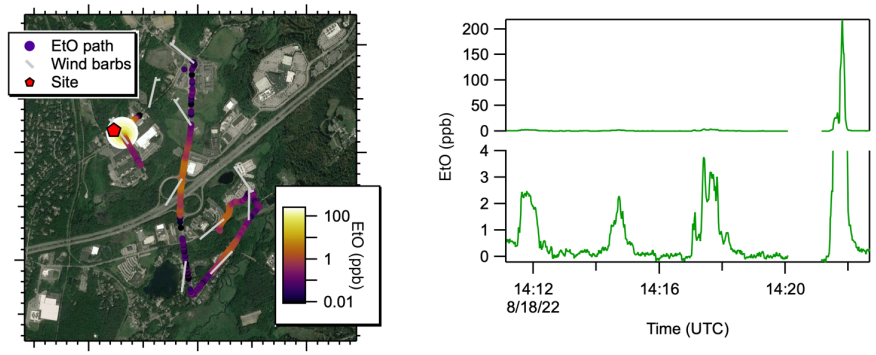

We follow the convention for wind barbs (e.g. https://www.weather.gov/hfo/windbarbinfo). We rephrase in the captions for SI figures and Figure 5: "[…] **with wind barbs tethered to the truck path, and feather end of the staff pointing into the wind.**"

Response to Reviewer Comments for

"Ethylene Oxide Monitor with Part-per-Trillion Precision for In-Situ Measurements"

by Yacovitch et al.

Reviewer comments are shown in blue, and responses are shown in black.

Reviewer comments "RC2"

https://doi.org/10.5194/amt-2022-294-RC2

Review of Yakovitch et al., AMTD

This is a nice concise paper that describes the TILDAS-FD-EtO analyzer for ethylene oxide.

This is a really difficult measurement (due to low conc and potential interferences) and the authors give a good description here.

The large enhancements from two Facilities observed at the lab are very interesting and chasing down those sources with the mobile lab is particularly impressive.

I only have a couple of minor comments below.

We thank the reviewer for their in-depth read and useful comments. We address them all below:

Line 7. I don't think the cell is 413m long. I think you mean a cell with a 413 m path length.
Indeed. We have reworded the sentence.

Line 55. Whats the cell pressure? Add it here.
We added the sentence: The sample pressure was maintained between 20 Torr (26 mbar) and 30 Torr (40 mbar) throughout the experiments described in this paper.

line 103. "averages down well" is something I would say but it is a bit informal. Maybe reword.
Agreed. We have reworded the sentence.

Line 129. Hysplit is a model not an engine.

We have reworded to model.

Line 152. I'm not sure this the best way to represent these statistics. Is the 18 ppt a general background for the hourly average in Fig 3?
Is the 22 ppt sd real signal or noise? Maybe include the averaging time? Maybe clarify what you explicitly mean here.

Yes, the 18 ppt is the average of the hourly data over the entire period. This was explained near original line 115 where these values are first mentioned. The instrument noise as a function of averaging time was explained in section Instrument Performance.

We have clarified further by adding the following sentence in Section Ambient Measurements: The standard deviations given reflect the combination of instrument noise as described above and the variability of EtO in ambient air.

We have also modified Figure 3 and added a box plot to it. This box plot shows the monthly median and percentiles. Furthermore, Figure S3 was added to show histograms of winter/spring and summer hourly average EtO values.

I think Fig S1 is especially helpful to the discussion. Would you consider moving it (or something similar) to the main text?

We have decided to leave this figure in the supplemental information.

Supplemental Information:
Ethylene Oxide Monitor with Part-per-Trillion Precision for In-Situ Measurements

Tara I. Yacovitch, Christoph Dyroff, Joseph R. Roscioli, Conner Daube, J. Barry McManus, Scott C. Herndon

Aerodyne Research, Inc. Billerica MA, 01821 USA

Correspondence to: Tara I. Yacovitch (tyacovitch@aerodyne.com)

Table of Contents

Deleted: 23

Deleted: 34

Deleted: 1312

Deleted: 1413

S1 Instrument

S1.1 Optical setup of single-laser dual with 413 m cell

The basis of our EtO monitor is our commercially available (Aerodyne Research Inc., 2022a, b) dual-laser tunable infrared direct absorption spectrometer (TILDAS-FD) platform, which in this case is equipped with a single mid-infrared interband-cascade laser (nanoplus GmbH). The highly divergent beam of this laser is collected and focused into a long-pathlength multipass cell using a sequence of reflective optics (McManus et al., 2015). A visible laser is co-aligned using a dichroic mirror to aid the optical alignment of the system.

For the system described herein, we use a multipass cell with 413 m optical pathlength and an active volume of 1.8 litres for continuous flow applications. The cell contains two mirrors with wavelength-specific high-reflectivity coating (reflectivity >99.8%) to minimize reflective losses of laser power during the > 800 reflections among the two mirrors. Upon exiting the cell, the laser beam is focused on a thermoelectrically cooled photovoltaic HgCdTe detector (Judson, J19 with transimpedance amplifier).

The laser is driven by electrical current while being maintained at a constant temperature. The in-house software TDLWintel provides a voltage ramp via a digital-to-analogue converter card (National Instruments). This ramp is translated into current via a low-noise laser driver (QCL-500, Wavelength Electronics). The laser temperature is maintained by an electronic temperature controller via the built-in thermoelectric element in the sealed laser housing. The detector signal is digitized using an analogue-to-digital convert card (National Instruments) and then handled by TDLWintel for processing.

The laser wavelength is scanned across a narrow wavelength interval near 3065 cm-1 approximately 1830 times per second. For every scan, the laser is on for the first 90% of the time, followed by a brief period where it is off for the remaining 10% of the time. The individual spectra are then averaged to a single spectrum every 1 second. This averaged spectrum is then processed in TDLWintel to derive the mixing ratio of EtO as well as of all other absorbers defined in the spectroscopic fit at 1 Hz in real time.

Spectra are defined by absorption signal, a polynomial spectral baseline (full light, no absorption), as well as signal during the off period (no light, complete absorption). The latter two components are used to normalize the measured spectra onto the transmission scale (0 – 1).

The wavelength scale of the laser scan is determined by periodically analyzing the interference spectrum of a Germanium etalon. The derived wavelength scale is then further refined measuring a high-concentration ethylene (C_2H_4) spectrum from a reference cell built into an optional beam path in the spectrometer optics. Wavelength drift is mitigated by locking the laser to a strong H_2O line in the sample spectrum using an active feedback loop controller realized in software.

S1.2 Flow system

Sample gas is drawn through the multipass cell at a reduced pressure of 20 Torr (27 hPa) using a vacuum pump downstream of the instrument and an upstream pressure controller. This reduced pressure is used to sharpen the absorption lines in the

Deleted: analysing

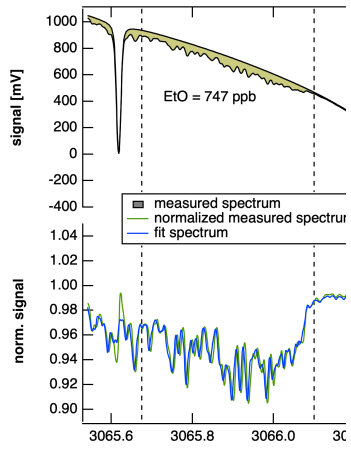

Deleted:
Figure S1. Summary spectrum for instantaneous Facility A measurement of 747 ppb. The top shows signal as a function of wavenumber, with EtO contributions highlighted in yellow. The bottom shows normalized measured (green) and fit (blue) spectrum. ¶

spectrum and provide the best compromise of spectroscopic selectivity and sensitivity. The gas-flow rate is typically around 3 – 5 slpm (slpm: standard litres per minute), resulting is a gas exchange rate of 1 Hz or better.

An overblow port is set up to deliver calibration gas or ultra-zero air. To prevent pressure disruptions, this port is tied into the inlet ~6 inches from the tip using a union tee. For humidity-matched zeroes, a parallel flow path is set up, with a length-matched piece of tubing and 6" by 1" scrubber cartridge isolated by two solenoid valves. We use a manganese dioxide/copper oxide catalyst as scrubber: Carulite 500® (Carus LLC), heated to 150 C. These valves actuate at the same time, pulling ambient air through the scrubber and providing near-humidity-matched zero air free of EtO.

Spectral backgrounding (or autobackgrounding) is done by intermittently and regularly measuring air free of EtO. A background spectrum is acquired and used to divide subsequent sample spectra, reducing the impact of drift due to instrumental effects like optical fringes and spectral baseline effects. Each background takes about 1 minute at 3 - 5 SLPM in order to flush out the cell, acquire clean spectra, and return to sampling.

S2 Calibration

The EtO-TILDAS instruments reports dry air mixing ratios that have been mathematically corrected for the dilution effects of water vapor, as well as for empirical water broadening effects. At the ambient humidity measured, these effects are expected to be < 3%.

In a typical calibration, 50-500 sccm of an EtO standard at 1 ppm EtO is delivered via an Alicat mass flow controller to a ½" overblow line connected via a T-fitting 6 inches from the inlet tip. Calibrations are done either by standard addition to humid ambient air, with a known total inlet flow rate (3 – 10 SLPM) or via dilution into a known flow (3-10 SLPM) of ultra-zero air delivered by a second Alicat mass flow controller. Humid standard additions are preferred, as they most closely resemble sampling conditions.

Standard concentrations were calculated based on the known calibration tank concentrations and the known system flows. Calibration factors (m) consist of the slope of a linear plot of measured EtO vs standard EtO, where true_conc = *m* * meas_conc.; when applying these calibration factors, divide the raw reported EtO by the slope. Two example calibration curves are shown below. Note that during dry calibrations in UZA, the EtO intercept is fixed to 0; during standard additions it is floated to account for potential ppt-level background concentrations. Example calibration curves for a dry (left) and humid (right) calibration are shown below. The 2021 Airgas calibration tank used in these results is shown in Figure S2.

Deleted: Figure S2Figure S3

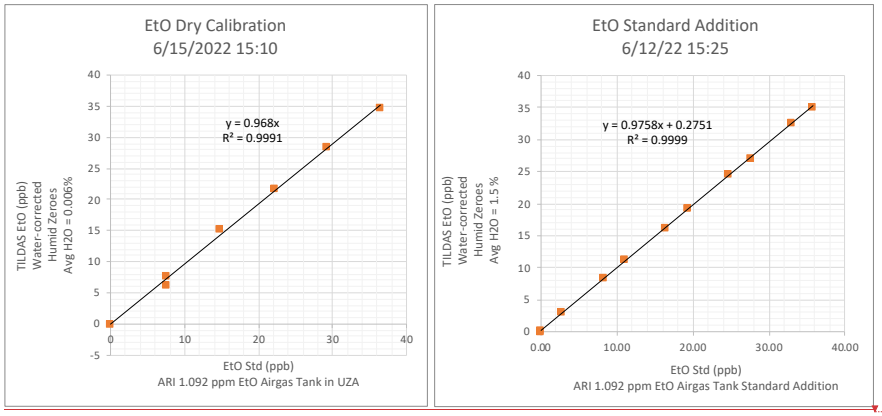

Figure S1. Example dry dilution (left) and standard addition (right) calibrations for EtO.

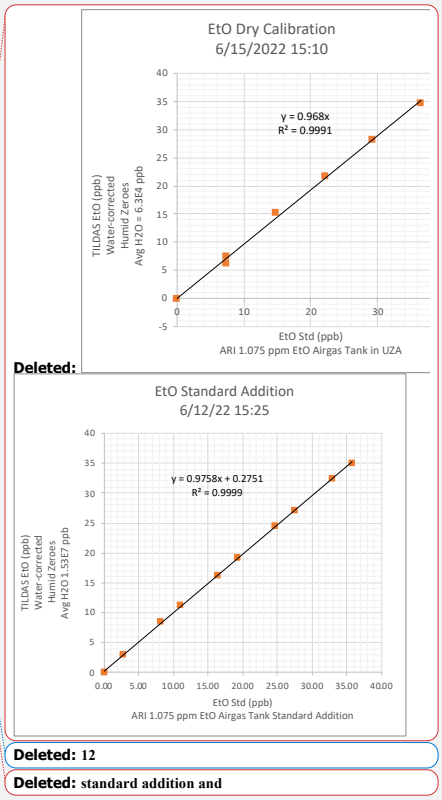

Deleted:

Deleted: 12

Deleted: standard addition and

Airgas
an Air Liquide company

Airgas Specialty Gases
Airgas USA, LLC
6141 Easton Road
Bldg 1
Plumsteadville, PA 18949
Airgas.com

CERTIFICATE OF ANALYSIS

Grade of Product: CERTIFIED STANDARD-SPEC

Part Number:	X03NI99C15A05D3	Reference Number:	160-401988504-1
Cylinder Number:	CC68617	Cylinder Volume:	144.3 CF
Laboratory:	124 - Plumsteadville - PA	Cylinder Pressure:	2015 PSIG
Analysis Date:	Dec 31, 2020	Valve Outlet:	350SS
Lot Number:	160-401988504-1		

Product composition verified by direct comparison to calibration standards traceable to N.I.S.T. weights and/or N.I.S.T. Gas Mixture reference materials.

ANALYTICAL RESULTS

Component	Req Conc	Actual Concentration (Mole %)	Analytical Uncertainty
ETHANE	1.000 PPM	1.075 PPM	+/- 5%
ETHYLENE OXIDE	1.000 PPM	1.092 PPM	+/- 5%
NITROGEN	Balance		

Approved for Release

Figure S2. Airgas calibration tank containing ethane and ethylene oxide at 1 ppm.

Deleted: 23

Table S1. Summary calibration factors for humid vs dry calibrations of ARI's Airgas tank X03NI99C15A05D3 over a week-long period

Statistics	Humid Standard Additions	Dry Calibrations
Average	0.981	0.999
StdDev	0.014	0.021
95% error	0.045	0.068
% error	4.6%	6.8%
1 ppb EtO would be corrected to	1.020	1.001

Deleted: *

Table S2. Summary calibration factors for all calibrations of ARI's Airgas tank X03NI99C15A05D3 (both humid and dry) over a week-long period

Statistics	Average all ARI Tank
Average	0.979
StdDev	0.037
Count	9
95% error	0.084
% error	8.6%
1 ppb EtO would be corrected to	1.021
Certified Tank Conc (ppm)	1.092 ± 5%
Measured Tank Conc (ppm)	1.069 ± 8.6%

S3 Ambient Measurements

S3.1 Statistics for Ambient Measurements

Averages of the full time series, and of winter/spring (Feb 2022 – April 30 2022) and summer (July 1, 2022 – Aug 4, 2022) averages of the 1hr data shown in Figure 3 of the Manuscript are listed in Table S3 below. To understand whether the Winter/Spring and summer averages are significantly different, we compute the standard error of the mean (SEM), where SEM = SD/sqrt(N). We also include and propagate through a 5% error due to calibration uncertainty, yielding propagated error bars of 1-2 ppt for the averages. The upper and lower confidence limits at 95% confidence (UL and LL) are listed for winter/spring

Deleted: Table S3Table S3

and summer averages. The winter UL of 14 ppt does not overlap the summer LL of 31 ppt, leading us to conclude, using these Gaussian statistics, that the averages are significantly different at the 95% confidence level.

Since these statistics do include the small number of plumes observed, we also show histograms and Gaussian fits of the data in Figure S3. The Gaussian peaks occur at 12 ppt for the winter/spring and 32 ppt for summer, comparing well to the full averages computed in Table S3 of 12 ppt and 33 ppt, respectively, and do not alter the conclusions.

Deleted: Figure S3Figure S4

Deleted: Table S3Table S3

Table S3. Averages and statistics for 1hr ambient data shown in Figure 3 of the Manuscript, all values in ppb. "Winter/Spring" spans from February to April 30, 2022. "Summer" spans July to August 4, 2022. The standard Deviation (SD), number of 1hr averages (N), Student's T statistic at 95% confidence (t), 95% error bars using the SD are listed. Additional statistics for the mean are included: the standard error of the mean (SEM), 95% error bars for the average using the SEM, estimated error bars assuming a 5% calibration uncertainty, the resulting propagated error, and the resulting 95% Lower Limit (LL) and Upper Limit (UL) for winter and summer averages.

	Avg	SD	N	t, 95% Conf	95% Error using SD	SEM	95% error from SEM	Error 5% Cal. Uncert	Prop-agated error	LL	UL
All Data shown in Manuscript Figure 3 Error! Reference source not found.	0.018	0.022	2610	1.961	0.043	0.0004	0.0008	0.001	0.001	0.017	0.020
Winter/ Spring (ending 30 April)	0.012	0.023	1613	1.961	0.044	0.0006	0.0011	0.001	0.001	0.011	0.014
Summer (beginning 1 July)	0.033	0.013	485	1.965	0.026	0.0006	0.0012	0.002	0.002	0.031	0.035

Deleted: April

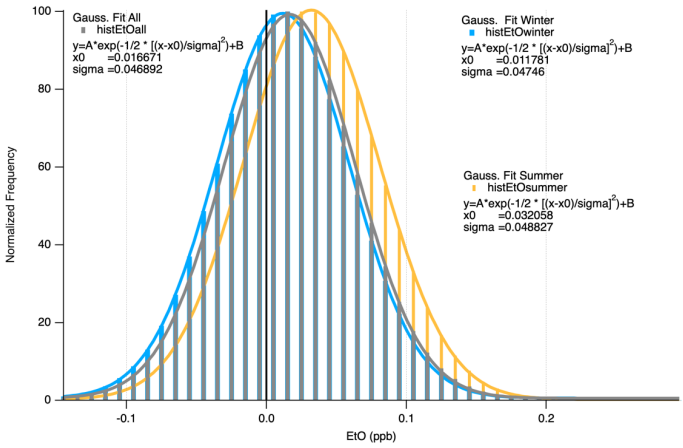

Figure S3. Histogram of 1hr average data in winter/spring (blue), summer (yellow) and all ambient measurements (grey).

Deleted: 34

S3.2 Hysplit Back Trajectories

The back trajectory analysis was computed using the National Oceanic and Atmospheric Administration (NOAA) Air Resources Laboratory (ARL) Hybrid Single-Particle Lagrangian Integrated Trajectory model (HYSPLIT). The work depicted here in the SI used the web-based model with default options. The parameters for the run are noted in the figure legend. This work involved straightforward back trajectory calculation. Although HYSPLIT is capable of a rigorous source-receptor analysis, the physical correspondence noted below has been performed 'by eye', not via a quantitative attribution. Details of the NOAA/ARL HYSPLIT model (Rolph et al., 2017; Stein et al., 2015) can be found in the cited sources or at the primary website (https://www.arl.noaa.gov/hysplit/).

Deleted:

Deleted:

Deleted:

Deleted:

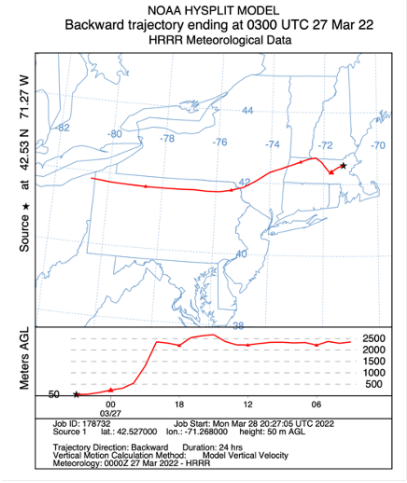

Figure S4. Back trajectory simulation for the EtO event on 3/27/2022. (NOAA Air Resources Laboratory)

Deleted: 45

150

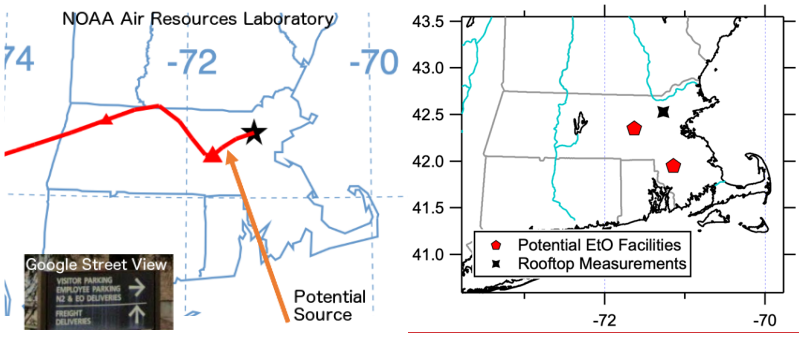

Figure S5. Left: Detail of back trajectory (NOAA Air Resources Laboratory). The orange arrow indicates location of one potential EtO source in the state. A roadside-view of this facility's signage is inset (© Google Street View), with "EO deliveries" noted. Right: Location of rooftop measurements (black marker) and two potential EtO facilities (red markers) in the state of Massachusetts. Map outlines from NOAA (NOAA, 2013).

Deleted: 56

155

S4. Mobile Measurements

S4.1 Facility A measurements

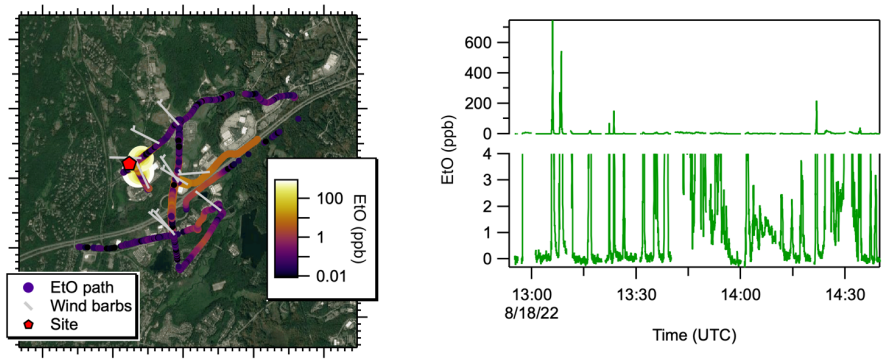

Figure S6. Morning summary data downwind of Facility A. A map (left) shows AML path colored by EtO concentration, with wind barbs tethered to the truck path, and feather end of the staff pointing into the wind. Time series show EtO concentrations zoomed to 0-4 ppb (bottom right) and at full scale (top right). Map underlay: Google, © 2022 CNES / Airbus, Landsat / Copernicus, MassGIS, Commonwealth of Massachusetts EOEA, Maxar Technologies, USDA/FPAC/GEO

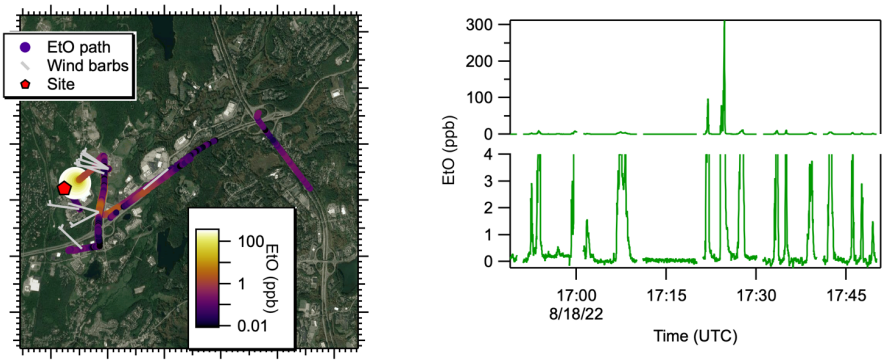

Figure S7. Afternoon Summary data downwind of Facility A. A map (left) shows AML path colored by EtO concentration, with wind barbs pointing into the wind. Time series show EtO concentrations zoomed to 0-4 ppb (bottom right) and at full scale (top right). Map underlay: Google, © 2022 CNES / Airbus, Landsat / Copernicus, MassGIS, Commonwealth of Massachusetts EOEA, Maxar Technologies, USDA/FPAC/GEO

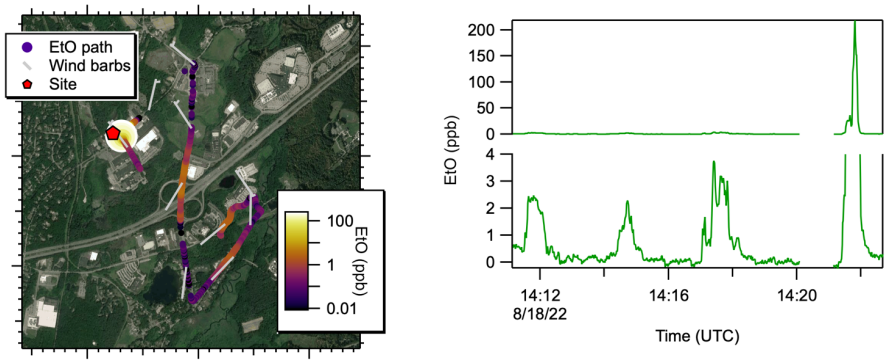

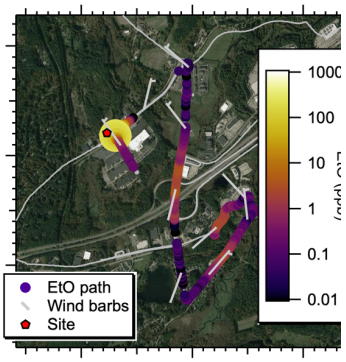

Deleted:

Figure S8. Detail of Morning Transect Downwind of Facility A. A map (left) shows AML path colored by EtO concentration (log scale), with wind barbs tethered to the truck path, and feather end of the staff pointing into the wind. Time series show EtO concentrations zoomed to 0-4 ppb (bottom right) and at full scale (top right). Map underlay: Google, © 2022 CNES / Airbus, Landsat / Copernicus, MassGIS, Commonwealth of Massachusetts EOEA, Maxar Technologies, USDA/FPAC/GEO

Deleted: 89

Spatial averaging was done for all data collected on 8/18/2022 at Facility A. Bins are 100m x 100m in size.

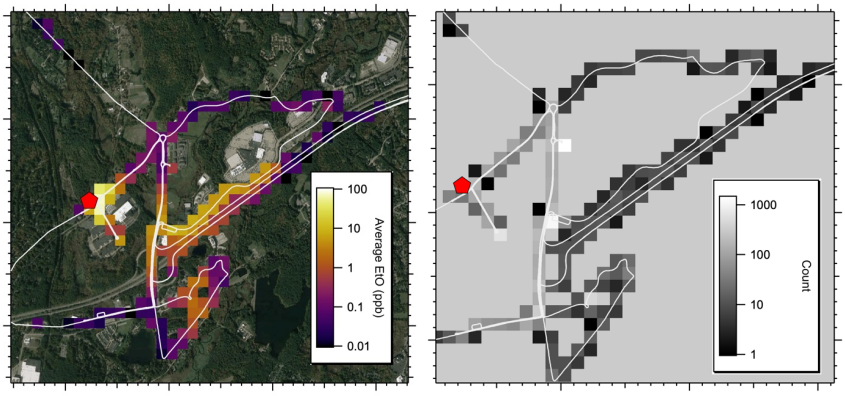

Figure S9. Binned average EtO concentrations (log scale) downwind of Facility A (left) along with data point count (right). The facility is located at the red marker. Wind was consistently from the North-West during these measurements. Map underlay: Google, © 2022 CNES / Airbus, Landsat / Copernicus, MassGIS, Commonwealth of Massachusetts EOEA, Maxar Technologies, USDA/FPAC/GEO

Deleted: 910

The archived spectra can be used to unambiguously spectrally fingerprint the EtO observed at these facilities. For example, Figure S10 (top) shows raw measured signal out of plume (black) overlaid on signal in-plume (gold area) at Facility A. In Figure S10 (bottom), we manually divide the in-plume and out-of-plume spectra to reveal the spectral signature of EtO. Line scars at the positions of the water lines are observable (green spikes) due to slight variations in laser peak position. The blue line is a transmission simulation of EtO only, and clearly matches the experimental result.

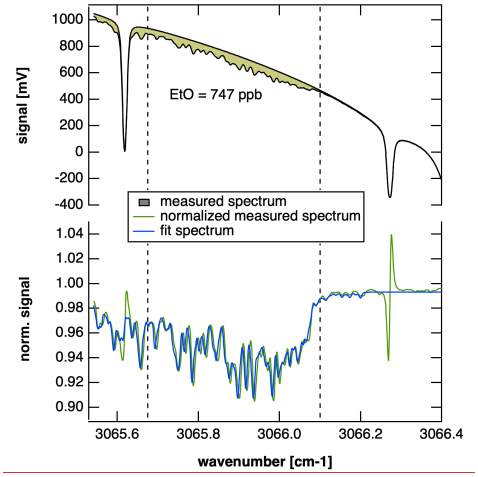

Figure S10. Summary spectra comparing instantaneous Facility A measurement of 747 ppb (in-plume, gold) to an out-of plume spectrum. The top shows signal as a function of wavenumber, with EtO contributions highlighted in yellow. The bottom shows a divided spectra in-plume/out-of-plume (green) and transmission simulation of EtO only.

Deleted: Figure S10

Deleted: Figure S10

Formatted: Normal

S4.2 Facility B Measurements

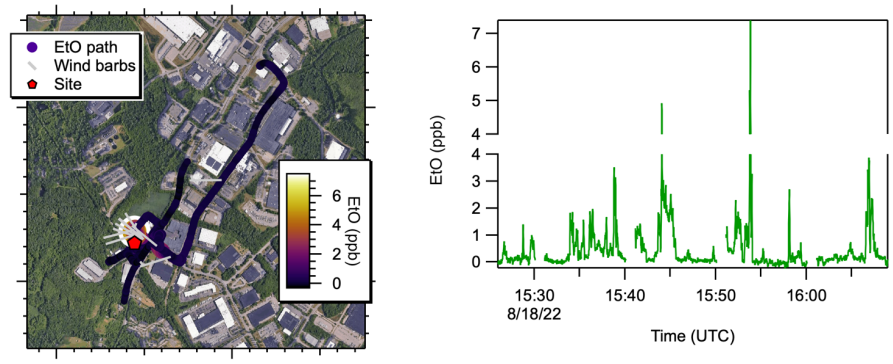

Figure S11. Full Summary time series downwind of Facility B. A map (left) shows AML path colored by EtO concentration, with wind barbs tethered to the truck path, and feather end of the staff pointing into the wind. Time series show EtO concentrations zoomed to 0-4 ppb (bottom right) and at full scale (top right). Map underlay: Google, © 2022 CNES / Airbus, Landsat / Copernicus, MassGIS, Commonwealth of Massachusetts EOEA, Maxar Technologies, RIGIS, USDA/FPAC/GEO

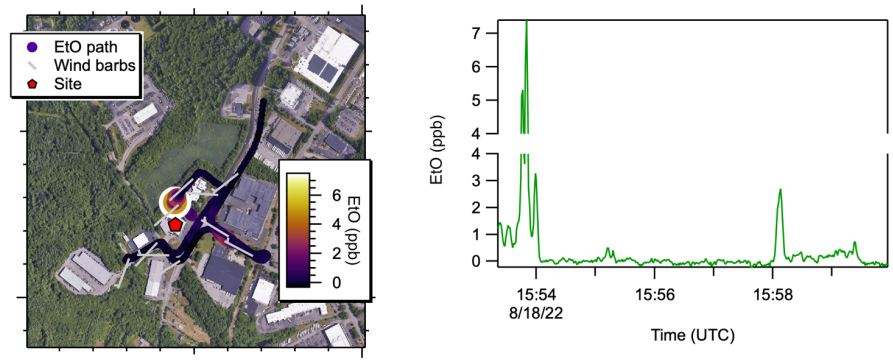

Figure S12. Detail of time series downwind of Facility B. A map (left) shows AML path colored by EtO concentration, with wind barbs tethered to the truck path, and feather end of the staff pointing into the wind. Time series show EtO concentrations zoomed to 0-4 ppb (bottom right) and at full scale (top right). Map underlay: Google, © 2022 CNES / Airbus, MassGIS, Commonwealth of Massachusetts EOEA, Maxar Technologies, RIGIS, USDA/FPAC/GEO

Spatial averaging was done for all data collected on 8/18/2022 at Facility B. Bins are 100m x 100m in size.

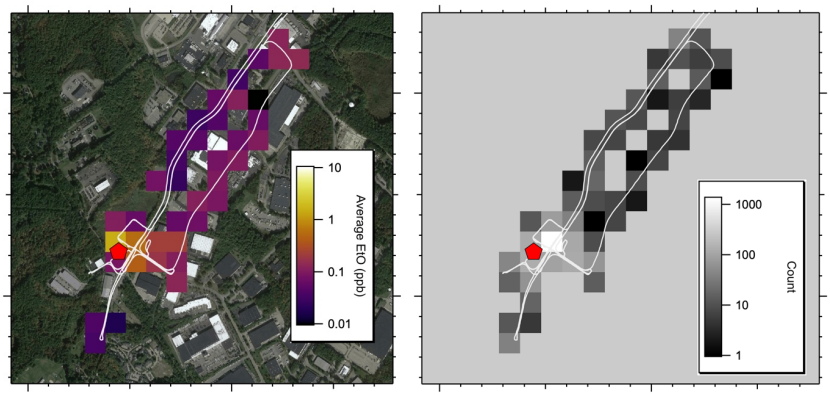

Figure S13. Binned average EtO concentrations downwind of Facility B (left) along with data point count (right). The facility is located at the red marker. Wind was from the West during these measurements. Map underlay: Google, © 2022 CNES / Airbus, MassGIS, Commonwealth of Massachusetts EOEA, Maxar Technologies, RIGIS, USDA/FPAC/GEO

References

Aerodyne Research Inc.: Laser trace gas and isotope analyzers, 2022a. https://www.aerodyne.com/product/laser-trace-gas-and-isotope-analyzers/, last

Aerodyne Research Inc.: TILDAS compact single laser ethylene oxide analyzer, 2022b. https://www.aerodyne.com/wp-content/uploads/2022/01/EthyleneOxide.pdf, last

McManus, J. B., Zahniser, M. S., Nelson, D. D., Shorter, J. H., Herndon, S. C., Jervis, D., Agnese, M., McGovern, R., Yacovitch, T. I., and Roscioli, J. R.: Recent progress in laser-based trace gas instruments: Performance and noise analysis, Applied Physics B, 119, 203-218, 10.1007/s00340-015-6033-0, 2015.

NOAA: Global self-consistent, hierarchical, high-resolution geography database (GSHHG): Version 2.2.0, 2013.

Rolph, G., Stein, A., and Stunder, B.: Real-time environmental applications and display system: Ready, Environmental Modelling & Software, 95, 210-228, https://doi.org/10.1016/j.envsoft.2017.06.025, 2017.

Stein, A. F., Draxler, R. R., Rolph, G. D., Stunder, B. J. B., Cohen, M. D., and Ngan, F.: NOAA's HYSPLIT atmospheric transport and dispersion modeling system, Bulletin of the American Meteorological Society, 96, 2059-2077, 10.1175/bams-d-14-00110.1, 2015.